

Supplementary Figures for the Main Modeling

Andrea K. Barreiro[#] ; Shree Hari Gautam[‡] ; Woodrow L. Shew[‡] ; Cheng Ly[†]

Department of Mathematics, Southern Methodist University, Dallas, TX 75275 U.S.A.

‡Department of Physics, University of Arkansas, Fayetteville, AR 72701 U.S.A.

*†Department of Statistical Sciences and Operations Research, Virginia Commonwealth University,
Richmond, VA 23284 U.S.A.*

* E-mail: abarreiro@smu.edu ; shgautam@uark.edu; woodrowshew@gmail.com ; CLy@vcu.edu

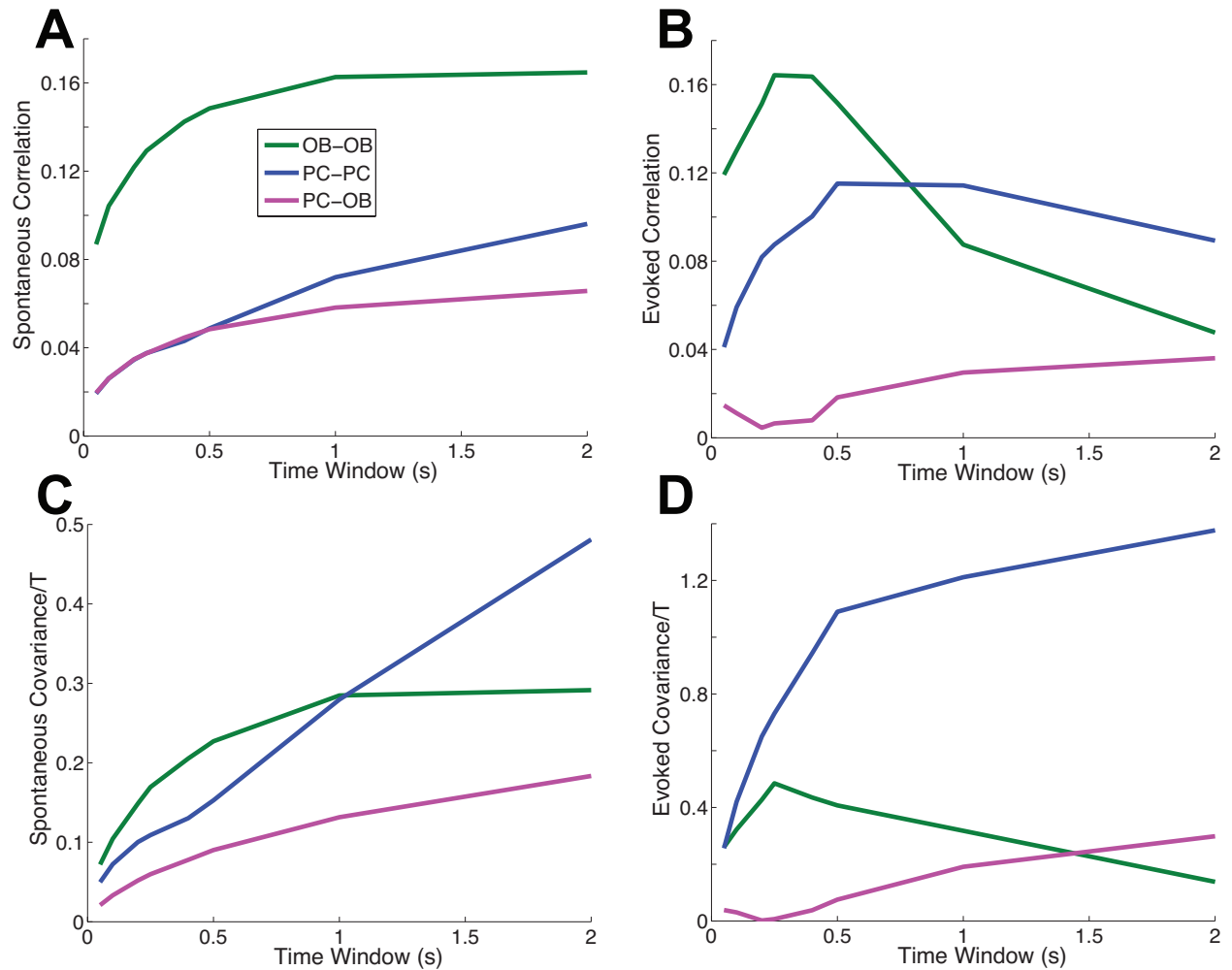


Figure S9: Cross-region correlations are smaller than within-region correlations. The experimental data shows that the PC-OB correlation and covariance is small (on average) compared to both OB and PC. A: In the spontaneous state, the (average) Fano Factor of the PC cells is larger than the OB cells. B: In the evoked state, the (average) variance of spike counts of OB cells is larger than the PC cells; here, we have divided by the time window for illustration purposes (which obviously does not change the relationship). In both A and B, there are 73 PC cells and 41 OB cells. C: In the evoked state, the (average) OB covariance is larger than the PC covariance. D: The evoked variance among OB cells is larger than the spontaneous OB variance. In C and D, the covariances were scaled by the time window for illustration purposes, and there were 1298 pairs of PC cells and 406 pairs of OB cells.

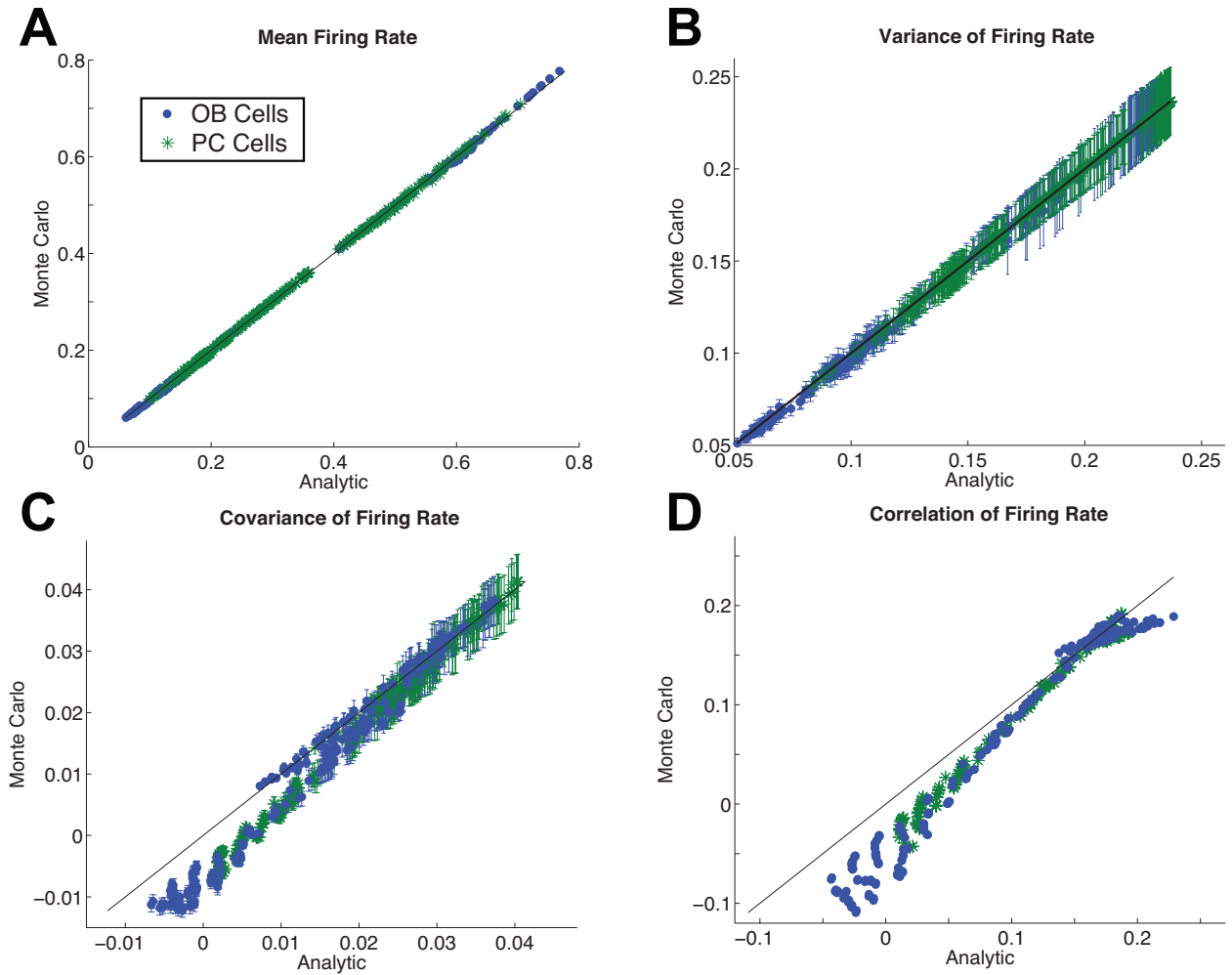
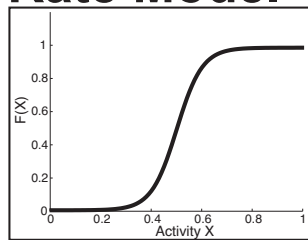


Figure S10: **Fast analytic approximation accurately captures statistics of a multi-population firing rate model.** Comparing the results of the fast analytic approximation to Monte Carlo simulations from 100 randomly selected parameters in the 6 equation rate model: $-2 \leq gIO < 0$, $-2 \leq gIP < 0$, $0 < gEO \leq 2$, $0 < gEP \leq 2$. Comparing 4 important firing rate statistics on a cell by cell basis (i.e., not the average across the population); the statistics for the activity X_j are just as accurate (not shown). A: The mean firing rate $F(X_j)$. B: The variance of the firing rate $Var(F(X_j))$. C: The covariance of the firing rate between OB pairs and PC pairs (we do not focus on OB–PC pairs): $Cov(F(X_j), F(X_k))$. D: The correlation of the firing rate between OB and PC pairs: $\rho = Cov(F(X_j), F(X_k)) / \sqrt{Var(F(X_j))Var(F(X_k))}$. The fast analytic approximation is accurate (dots lie on the diagonal line). Error bars are shown in B and C, representing 95% confidence intervals assuming a normal distribution for finite number of realizations, or 1.96 standard deviations above and below the mean.

Schematic of Minimal Rate Model



Correlated Background Noisy Inputs

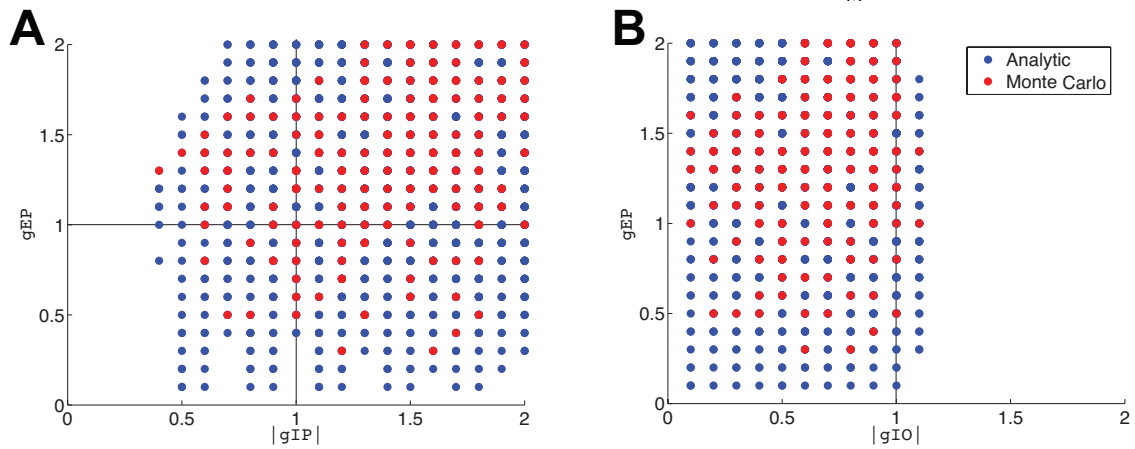
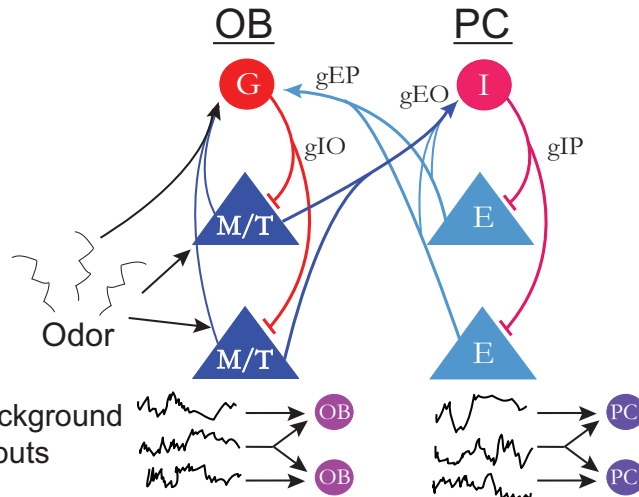


Figure S11: **Experimental observations constrain conductance parameters in analytic model.** The final 2 relationships between the 4 conductance parameters from the fast analytic theory for the rate model not shown in the main text with $F(X) = \frac{1}{2}(1 + \tanh((X - 0.5)/0.1))$. A: Both gEP and $|gIP|$ are relatively large. B: $|gIO|$ is relatively small.

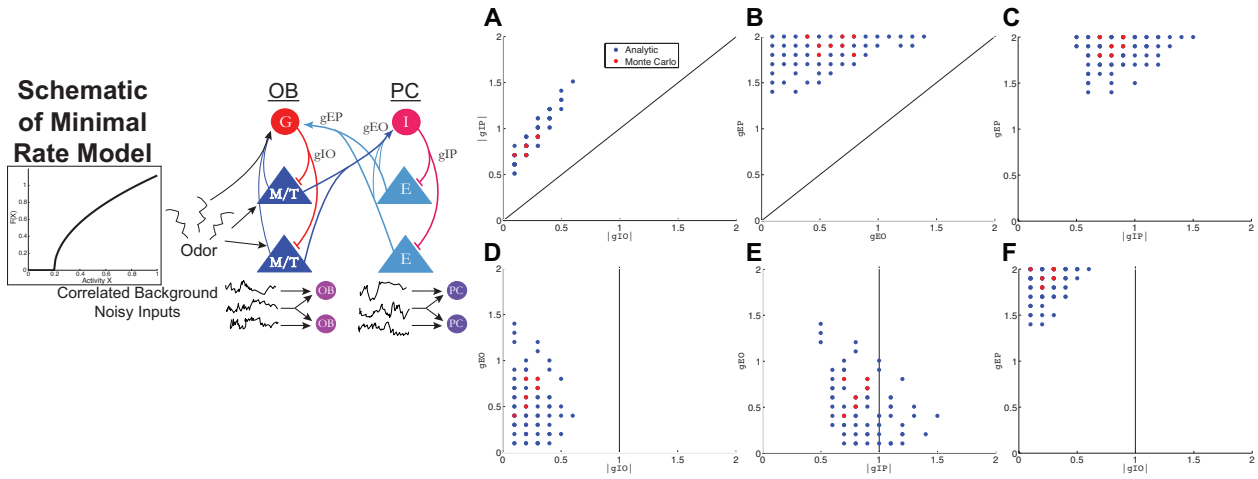


Figure S12: **Analytic approximation results are robust to choice of transfer function.** The results of the fast analytic theory for the rate model using a truncated square root transfer function $F(X) = 1.25\sqrt{X - 0.2}H(X - 0.2)$ are qualitatively similar to the results with the more common sigmoidal function in the main text. Here we have omitted the E to I connections within OB and PC because it does not qualitatively change the results. A: The inhibitory conductance within the PC population $|g_{IP}|$ is larger than in the OB population g_{OP} . B: The excitatory conductance from PC to OB g_{EP} is generally larger than OB to PC g_{EO} . C: Both g_{EP} and $|g_{IP}|$ are relatively large. D: $|g_{IO}|$ is relatively small. E: $|g_{IP}|$ is relatively large. F: Again, $|g_{IO}|$ is relatively small.

Full Spiking Model, μ to PC fixed in Spon./Evoked

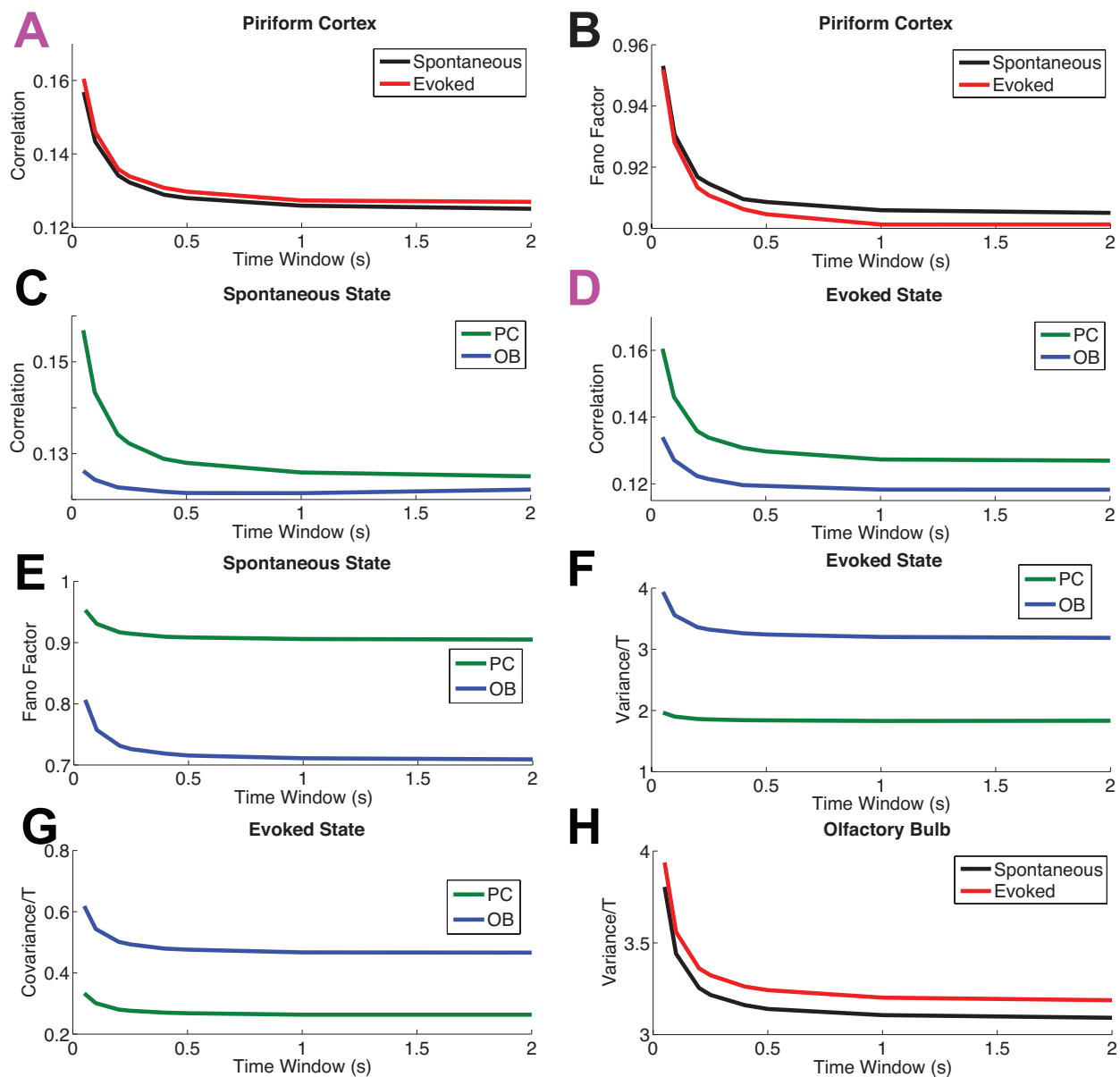


Figure S13: **Mean input to PC must increase in the evoked state.** Showing the results of the full LIF spiking model when the mean input to PC is the same in spontaneous and evoked states: $\mu_{PC} = 0$. The rest of the parameters are the same as in Figure 6 (see main text). The firing rates are: $\nu_{OB}^{Sp} = 5.5 \pm 4.6$, $\nu_{OB}^{Ev} = 5.7 \pm 4.6$, $\nu_{PC}^{Sp} = 2.096 \pm 2.6$, and $\nu_{PC}^{Ev} = 2.13 \pm 2.6$, which barely satisfies the constraint from the experimental data that $\nu_{PC}^{Ev} > \nu_{PC}^{Sp}$. The 8 panels show the constraints on the 2nd order spiking statistics in the same format as in Figure 6 of the main text. The evoked PC correlations decrease but not enough; panels A and D with magenta coloring show the 2 constraints that are violated.

Full Spiking Model, Test 1: $g_{IP} < g_{IO}$

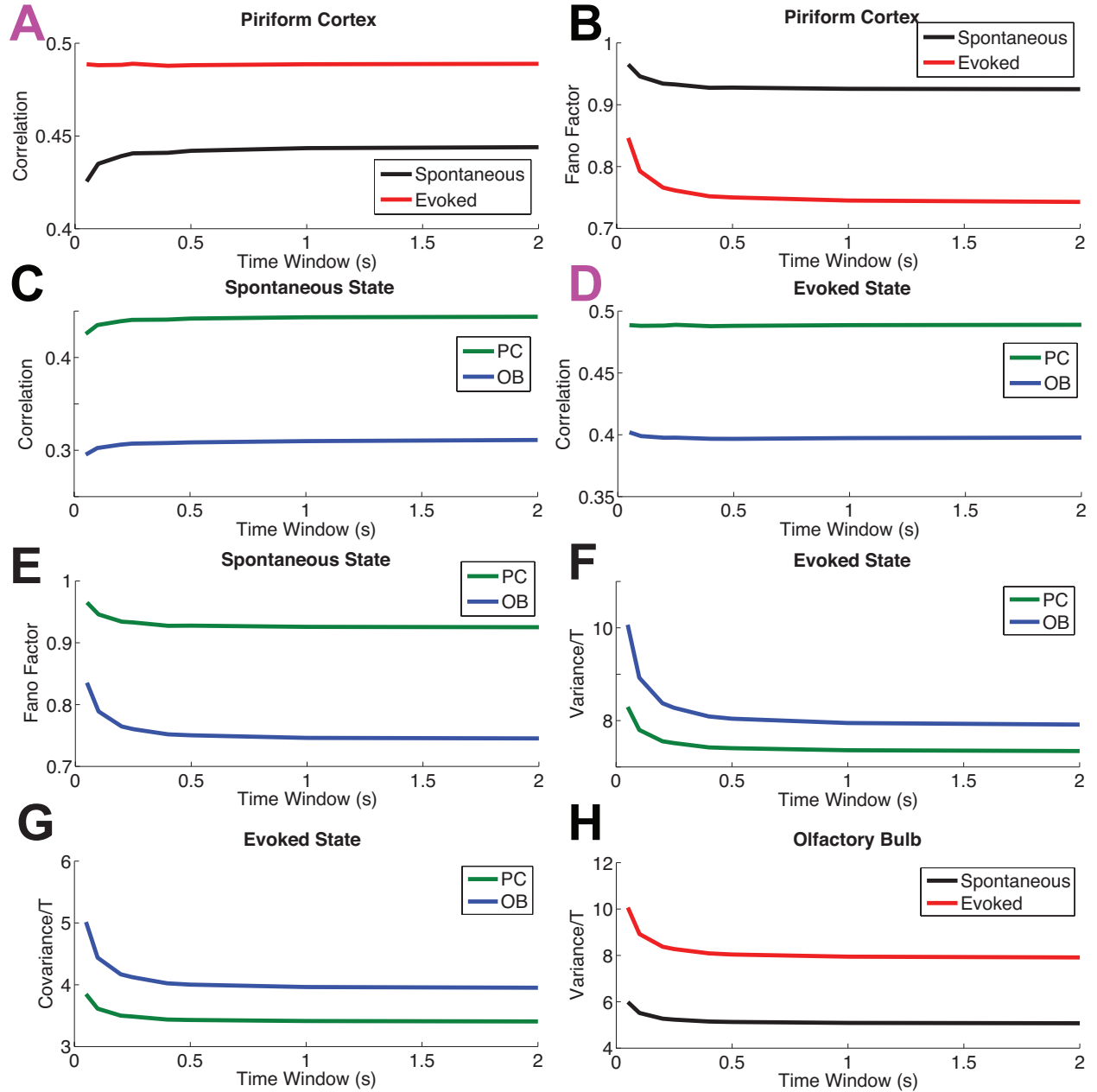


Figure S14: **Violating derived relationship $|g_{IO}| < |g_{IP}|$ results in statistics that are inconsistent with experimental observations.** Showing the results of the full LIF spiking model when $g_{IP} < g_{IO}$; specifically, we set $g_{IP} = 7$ and $g_{IO} = 20$ and set the values of the rest of the parameters to those used in Figure xxx (see main text). The firing rates are: $\nu_{OB}^{Sp} = 7.82 \pm 5.64$, $\nu_{OB}^{Ev} = 13.42 \pm 8.36$, $\nu_{PC}^{Sp} = 3.8 \pm 2.82$, and $\nu_{PC}^{Ev} = 9.67 \pm 6.36$. The 8 panels show the constraints on the 2nd order spiking statistics in the same format as in Figure xxx of the main text. Two constraints are violated; the panels with magenta letters (i.e., A, D) are constraints that are violated.

Full Spiking Model, Test 2: $g_{EP} < g_{EO}$

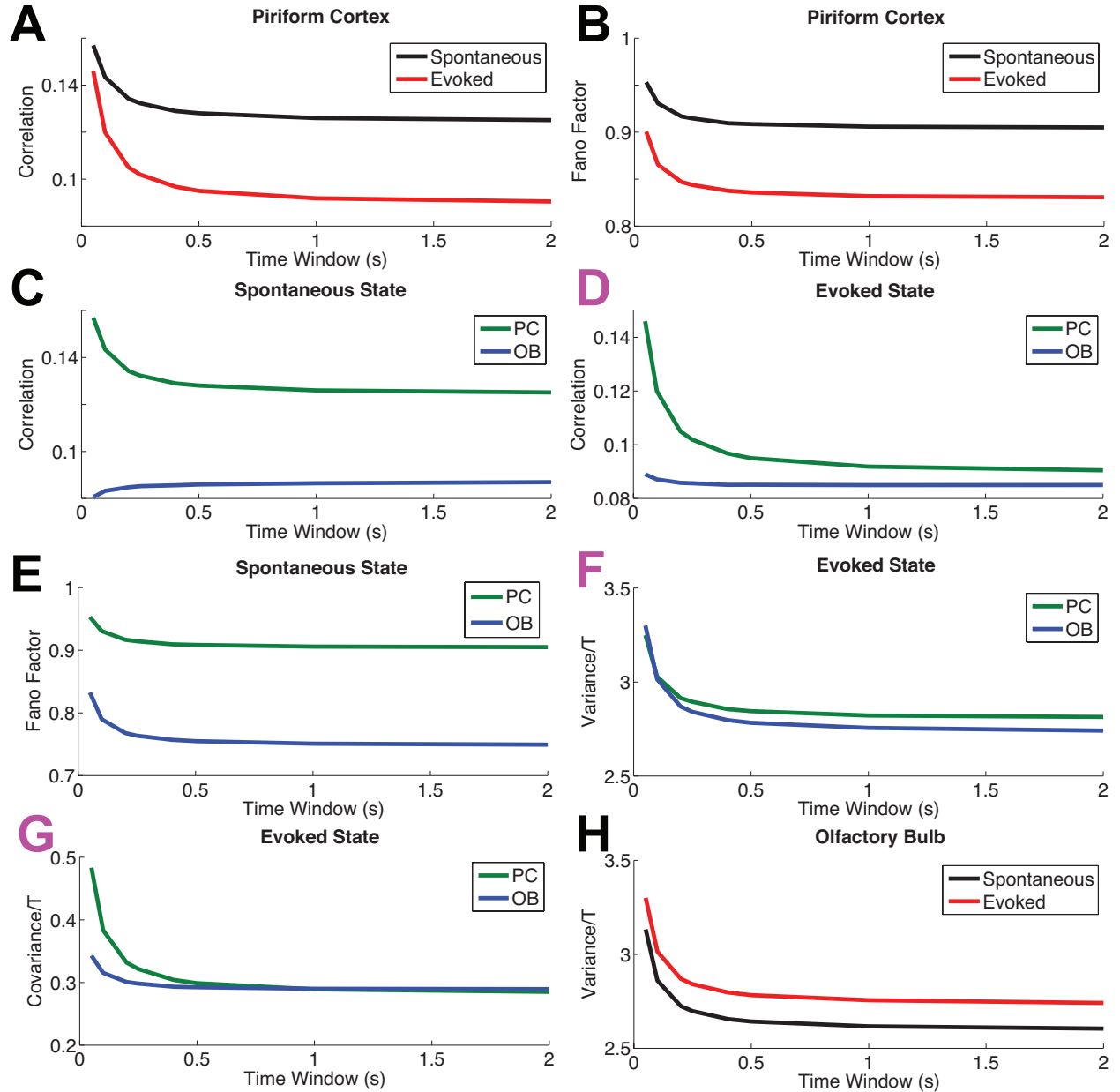


Figure S15: **Violating derived relationship $g_{EP} > g_{EO}$ results in statistics that are inconsistent with experimental observations.** Showing the results of the full LIF spiking model when $g_{EP} < g_{EO}$; specifically, we set $g_{EP} = 1$ and $g_{EO} = 15$; we set the values of the rest of the parameters to those used in Figure 6 (see main text). The firing rates are: $\nu_{OB}^{Sp} = 4.42 \pm 4.09$, $\nu_{OB}^{Ev} = 4.63 \pm 4.01$, $\nu_{PC}^{Sp} = 2.1 \pm 2.64$, and $\nu_{PC}^{Ev} = 4.17 \pm 5.81$. The 8 panels show the constraints on the 2nd order spiking statistics. Three constraints are violated (D, F, G in magenta); note that in G the constraints are violated for small time windows and almost indistinguishable for large time windows.

Full Spiking Model, Test 3: gIP, gEP small

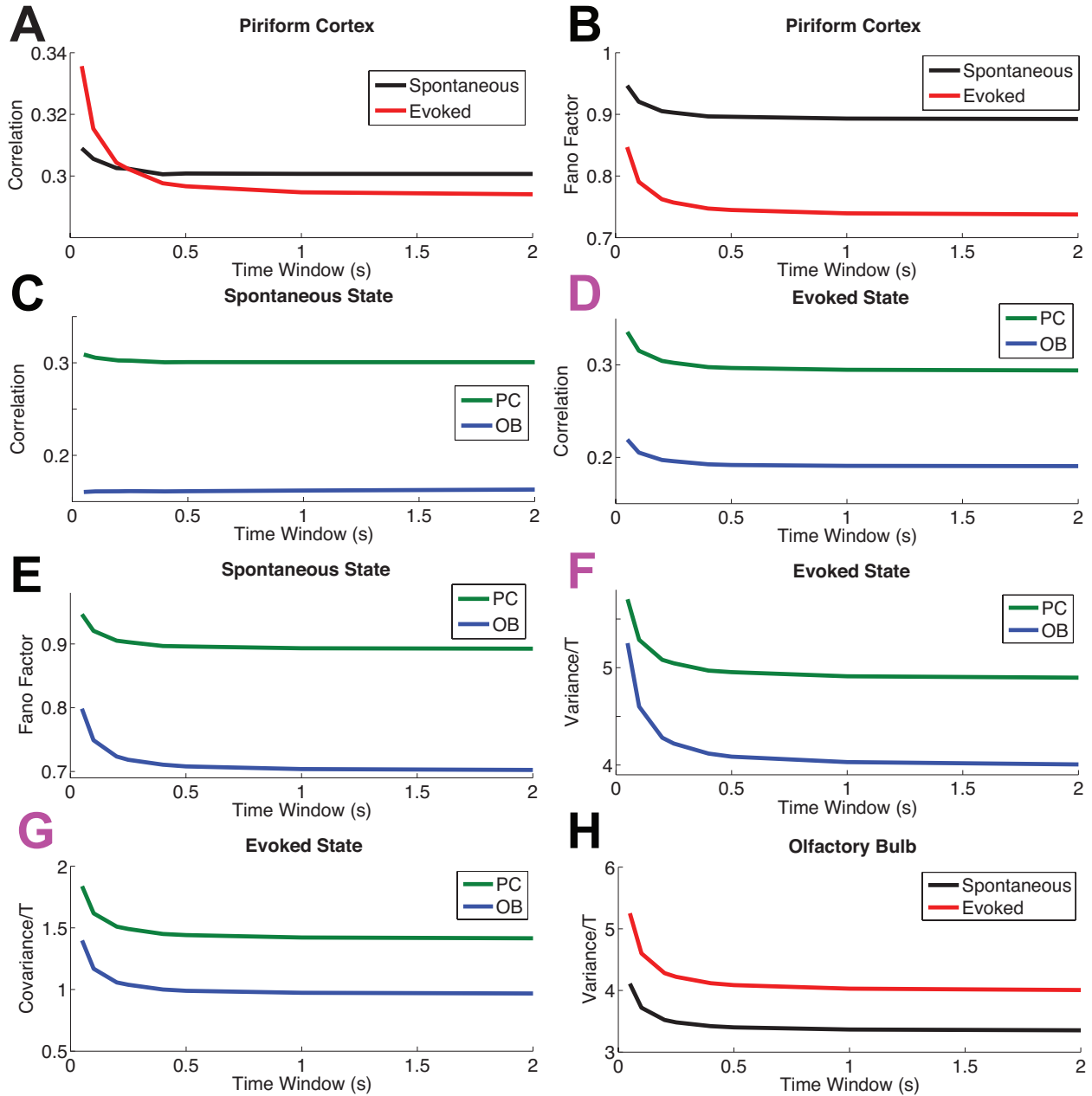


Figure S16: **Violating derived relationship $g_{EP}, g_{IP} \gg g_{EO}, g_{IO}$ results in statistics that are inconsistent with experimental observations.** Showing the results of the full LIF spiking model when g_{EP} and g_{IP} are both relatively small; specifically, we set $g_{EP} = 10$ and $g_{IP} = 10$ and set the values of the rest of the parameters to those used in Figure 6 (see main text). The firing rates are: $\nu_{OB}^{Sp} = 5.98 \pm 4.85$, $\nu_{OB}^{Ev} = 8.17 \pm 5.84$, $\nu_{PC}^{Sp} = 3.03 \pm 2.74$, and $\nu_{PC}^{Ev} = 6.95 \pm 6.1$. The 8 panels show the constraints on the 2nd order spiking statistics. The panels with magenta letters (i.e., D, F, G) are constraints that are violated.